Corrections to Strong-Stretching Theories

J. L. Goveas,*,†,‡ S. T. Milner,§ and W. B. Russel*,†

Department of Chemical Engineering, Princeton University, Princeton, New Jersey 08544, and Exxon Research & Engineering, Route 22 East, Annandale, New Jersey 08801

Received March 18, 1997; Revised Manuscript Received June 23, 1997[⊗]

ABSTRACT: We derive the strong-stretching approximation from the full partition function for diblock copolymer melts. Using a perturbation expansion for the free energy, with $(\chi N)^{-1/3}$ as the expansion parameter, we calculate the leading corrections to the asymptotic $\chi N \rightarrow \infty$ limit for the domain period and the free energy. The leading corrections to the free energy scale as $\log \chi N$. They arise from the entropy gain due to the wandering of chain ends over the domains and the entropy loss to localize the joints in the interfacial region.

I. Introduction

Diblock copolymers are produced by chemically linking two incompatible polymers (e.g., A and B). These copolymers exhibit ordering transitions from the molten homogeneous state to various microphase-separated states. The simplest of these ordered phases are one-dimensional lamellae, hexagonally packed arrays of cylinders, and body-centered cubic (bcc) arrays of spheres.[1] The diblock copolymer mean-field phase diagram may be described in terms of two parameters: χN, where N is the degree of polymerization of a single chain and χ is the Flory−Huggins parameter, and the relative composition of the two blocks (which we denote by f, the volume fraction of the A block).

It is useful to separate the mean field phase diagram into two limiting regimes. (i) Weak segregation. Here the melt is close to the ordering transition (which is at $(\chi N)_t = 10.5$ for copolymers with $f = 0.5$) and the composition profile of A and B blocks varies smoothly across the domains. The chains are only slightly perturbed from their random-walk configurations, and the interfaces separating A domains from B domains are wide. Both the domain period and the interfacial width scale as the radius of gyration of the copolymer chains. This regime has been successfully described by the theory of Leibler.[2] (ii) Strong segregation. For $\chi N \gg (\chi N)_t$, the interfaces become very sharp and narrow, separating almost pure A and B regions. The domain period scales as $aN^{2/3}$ (where a is the Kuhn length for a monomer), implying that the chains must be highly distorted from the Gaussian coil state. Analytical theories exist that postulate that the copolymer chains are strongly stretched perpendicular to the interface,[3,4] providing insight into the physics in this limit.

However, these so-called "strong-stretching" theories are strictly only valid in the limit $\chi N \rightarrow \infty$, and while the scaling predictions for the domain period have been verified for high values of χN,[5−7] most experiments are done at quite modest χN. Since there has been no rigorous derivation from the full partition function for strong stretching, it has not been clear at what point these theories break down, and only numerical solution of self-consistent field (SCF) equations has been able to handle intermediate values of χN (see, for example, refs 8 and 9). In addition, there have been both experimental and numerical indications that the domain period between weak and strong segregation has an apparent scaling exponent that is a higher power of N than 2/3.[8−10]

In this paper we shall derive the strong-segregation formalism via an asymptotic expansion for the free energy. This framework will provide a natural method for calculating finite χN corrections to the free energy and corresponding corrections to quantities such as the unit cell dimensions of microphases (e.g., the lamellar period).

Our starting point will be the mean-field equations for a copolymer melt, which we derive in section II (other derivations may be found in, for example, refs 11 and 12). We go on to separate the free energy into elastic and interfacial terms in section III and subsequently calculate the interfacial and elastic energy in sections IV and V. In section VI we expand the free energy in an asymptotic series and calculate the leading terms, in order to compare our predictions to numerical results in the literature. We comment on next-order corrections in section VII and conclude in section VIII.

II. Mean-Field Theory

Suppose we have a melt of N diblock copolymer chains, all of which are N monomers long, where the A and B blocks consist of N_A and N_B monomers, respectively. [We shall denote the block type by the subscript K, in which case the complementary block will be K'.] For simplicity we take the statistical segment lengths of both blocks to be equal to a and normalize the bulk densities ρ_0 to unity. We shall also assume that the melt is incompressible.

In the continuous limit, we can describe the path of the αth chain by the position coordinate $R^\alpha(s)$, where s is the arclength variable. The partition function for N such chains is then the weighted sum over all possible paths

$$Z = \frac{1}{N!}\prod_{\alpha=1}^{N}\int \mathrm{D}R^\alpha\, \delta(\hat{\rho}_\mathrm{A} + \hat{\rho}_\mathrm{B} - \rho_0) \times \exp\left[-\frac{3}{2a^2}\int_0^N \mathrm{d}s\left(\frac{\mathrm{d}R^\alpha}{\mathrm{d}s}\right)^2 - \chi\int \mathrm{d}x\,\frac{\hat{\rho}_\mathrm{A}\hat{\rho}_\mathrm{B}}{\rho_0}\right] \quad \text{(II.1)}$$

We shall set $k_\mathrm{B}T = 1$. This is a one-dimensional integral

† Princeton University.

‡ Present address: Materials Research Laboratory, University of California, Santa Barbara, California 93106.

§ Exxon.

⊗ Abstract published in *Advance ACS Abstracts,* August 15, 1997.

S0024-9297(97)00377-X CCC: $14.00

since in the transverse directions the chains are in their ideal, random-walk configurations. [The Gaussian integrals over the transverse directions do, of course, contribute to the partition function but are unimportant since we will later normalize Z by the partition function in zero field (see eq II.17).] We consider a system of length h and unit area.

The local density of K monomers is given by the operator

$$\hat{\rho}_K(x) = \sum_{\alpha=1}^{N} \int_0^N \mathrm{d}s\, \delta(x - R^\alpha(s))\theta_K(s) \qquad \text{(II.2)}$$

where $\theta_K(s)=1$ if s is a K monomer and zero otherwise.

All the chains interact through the A−B repulsion and the incompressibility constraint. We can convert the many-chain problem to a single-chain one by introducing fields through which the monomers interact, and replacing all local quantities by their averages in the fields.

We first deal with the incompressibility constraint by writing the delta-function in terms of the field $v(x)$ as

$$\delta(\hat{\rho}_\mathrm{A} + \hat{\rho}_\mathrm{B} - \rho_0) = \int \mathrm{D}v \exp[-\int \mathrm{d}x\, v(\hat{\rho}_\mathrm{A} + \hat{\rho}_\mathrm{B} - \rho_0)] \qquad \text{(II.3)}$$

Let us introduce the dimensionless density operator

$$\tilde{\rho}_K = \frac{\hat{\rho}_K}{\rho_0} \qquad \text{(II.4)}$$

[The bulk density for both species ρ_0 is just unity but we shall carry it along to make the dimensions obvious.] We treat the A−B interaction by introducing the auxiliary field $\eta(x)$

$$\exp[-\chi\rho_0 \int \mathrm{d}x\, \tilde{\rho}_\mathrm{A}\tilde{\rho}_\mathrm{B}] = \exp\left[-\frac{\chi\rho_0}{4}\int \mathrm{d}x\, [1 - (\tilde{\rho}_\mathrm{A} - \tilde{\rho}_\mathrm{B})^2]\right]$$

$$\propto \exp\left[-\frac{\chi\rho_0 h}{4}\right] \int \mathrm{D}\eta \times \exp[-\chi\rho_0 \int \mathrm{d}x\, \eta^2 - \chi\rho_0 \int \mathrm{d}x\, \eta(\tilde{\rho}_\mathrm{A} - \tilde{\rho}_\mathrm{B})] \qquad \text{(II.5)}$$

where we have used the identity $(\tilde{\rho}_\mathrm{A} + \tilde{\rho}_\mathrm{B})^2 - (\tilde{\rho}_\mathrm{A} - \tilde{\rho}_\mathrm{B})^2 = 4\tilde{\rho}_\mathrm{A}\tilde{\rho}_\mathrm{B}$. We can then write the partition function as

$$Z \propto \frac{1}{N!} \exp\left[-\frac{\chi\rho_0 h}{4}\right] \int \mathrm{D}v \int \mathrm{D}\eta\, P\{\eta,v\} \qquad \text{(II.6)}$$

where

$$P\{\eta,v\} = \prod_\alpha \int \mathrm{D}R^\alpha \exp\left[-\int_0^N \mathrm{d}s\, \frac{3}{2a^2}\left(\frac{\mathrm{d}R^\alpha}{\mathrm{d}s}\right)^2 - \chi\rho_0 \int \mathrm{d}x\, \eta^2 - \chi\rho_0 \int \mathrm{d}x\, \eta(\tilde{\rho}_\mathrm{A} - \tilde{\rho}_\mathrm{B}) - \int \mathrm{d}x\, v\rho_0[\tilde{\rho}_\mathrm{A} + \tilde{\rho}_\mathrm{B} - 1]\right] \qquad \text{(II.7)}$$

The chains now interact with each other only through the potentials $v(x)$ and $\eta(x)$. In order to evaluate the integrals over $v(x)$ and $\eta(x)$ by the saddle-point method we recast the partition function into the form

$$Z \propto \frac{1}{N!} \exp\left[-\frac{\chi\rho_0 h}{4}\right] \int \mathrm{D}v \int \mathrm{D}\eta \exp[\log P\{\eta,v\}] \qquad \text{(II.8)}$$

The saddle-point values of $v(x)$ and $\eta(x)$ are determined by $\delta P/\delta v = 0$ and $\delta P/\delta \eta = 0$ which imply the equations

$$\langle\tilde{\rho}_\mathrm{A}\rangle + \langle\tilde{\rho}_\mathrm{B}\rangle = 1 \qquad \text{(II.9)}$$

$$\langle\tilde{\rho}_\mathrm{A} - \tilde{\rho}_\mathrm{B}\rangle = -2\eta \qquad \text{(II.10)}$$

where we have defined the averages above as

$$\langle\cdot\rangle = \prod_\alpha \int \mathrm{D}R^\alpha\, (\cdot) \exp\left[-\int_0^N \mathrm{d}s\, \frac{3}{2a^2}\left(\frac{\mathrm{d}R^\alpha}{\mathrm{d}s}\right)^2 - \chi\rho_0 \int \mathrm{d}x\, \eta[\tilde{\rho}_\mathrm{A} - \tilde{\rho}_\mathrm{B}] - \int \mathrm{d}x\, v\rho_0[\tilde{\rho}_\mathrm{A} + \tilde{\rho}_\mathrm{B}]\right] \qquad \text{(II.11)}$$

Thus eqs II.9 and II.10 are really implicit in the constraint fields, with $v(x)$ being chosen such that the averaged local density is unity everywhere. From now on we will write the averaged local concentration as $\rho_K(x) = \langle\tilde{\rho}_K(x)\rangle$.

We may now write the partition function in terms of sums over single chains

$$Z \propto \frac{1}{N!} \exp[\rho_0(\int \mathrm{d}x\, v(x) + \chi \int \mathrm{d}x\, \rho_\mathrm{A}\rho_\mathrm{B})] \times \left(\int \mathrm{D}R \times \exp\left[-\int_0^N \mathrm{d}s\, \frac{3}{2a^2}\left(\frac{\mathrm{d}R}{\mathrm{d}s}\right)^2 - \int_0^N \mathrm{d}s\, v(R(s)) - \chi\rho_0 \int \mathrm{d}x\, \rho_\mathrm{B}\tilde{\rho}_\mathrm{A} - \chi\rho_0 \int \mathrm{d}x\, \rho_\mathrm{A}\tilde{\rho}_\mathrm{B}\right]\right)^N \qquad \text{(II.12)}$$

[Note that the factor of $\exp[-\chi\rho_0 h/4]$ is absent, since it cancels on substitution of eq II.10 into eq II.8.] Using eq II.2 for the local density and separating the integrals over A and B monomers

$$Z \propto \frac{1}{N!} \exp[\int \mathrm{d}x\, v(x) + \chi \int \mathrm{d}x\, \rho_\mathrm{A}\rho_\mathrm{B}] \times \left[\left(\int \mathrm{D}R \times \exp\left[-\int_0^{N_\mathrm{A}} \mathrm{d}s\, \frac{3}{2a^2}\left(\frac{\mathrm{d}R}{\mathrm{d}s}\right)^2 - \int_0^{N_\mathrm{A}} \mathrm{d}s[v(R(s)) + \chi\rho_\mathrm{B}(R(s))]\right]\right)^N\right] \times \left[\left(\int \mathrm{D}R \exp\left[-\int_{N_{\mathrm{A}+1}}^{N_\mathrm{B}} \mathrm{d}s\, \frac{3}{2a^2}\left(\frac{\mathrm{d}R}{\mathrm{d}s}\right)^2 - \int_{N_{\mathrm{A}+1}}^{N_\mathrm{B}} \mathrm{d}s\, [v(R(s)) + \chi\rho_\mathrm{A}(R(s))]\right]\right)^N\right] \qquad \text{(II.13)}$$

We now introduce the propagator $Q_K(x,s;x_1)$, which is the Boltzmann weight for a chain which starts at x_1 to reach a point x in s segments:

$$Q_K(x,s;x_1) = \int_{R(0)=x_1}^{R(s)=x} \mathrm{D}R \exp\left[-\int_0^s \mathrm{d}s'\, \frac{3}{2a^2}\left(\frac{\mathrm{d}R}{\mathrm{d}s'}\right)^2 - \int_0^s \mathrm{d}s'\, [v(R(s')) + \chi\rho_{K'}(R(s'))]\right] \qquad \text{(II.14)}$$

The propagator satisfies a modified diffusion equation (see for example ref 13 for a derivation) and is sym-

metric under the interchange of starting and ending points.

$$\frac{\partial Q_K}{\partial s} = \frac{a^2}{6}\frac{\partial^2 Q_K}{\partial x^2} - [v + \chi\rho_{K'}]Q_K \qquad \text{(II.15)}$$

and $Q_K(x, 0; x_1) = \delta(x - x_1)$.

We consider as a reference state the mixed homogeneous melt with the χ interaction switched off. Here the chains just execute random walks so we can write the propagator Q_{0K} as

$$Q_{0K}(x, s; x_1) = \left(\frac{3}{2\pi a^2 N_K}\right)^{1/2} \exp\left[\frac{-3(x - x_1)^2}{2a^2 N_K}\right] \qquad \text{(II.16)}$$

This allows us to calculate the partition function in zero field Z_0 so that

$$\frac{Z}{Z_0} = \exp[\int \mathrm{d}x\, \rho_0[v + \chi\rho_A\rho_B]]\tilde{Q}^N \qquad \text{(II.17)}$$

where

$$\tilde{Q}_1 = \frac{1}{h}\int \mathrm{d}x_A\, \mathrm{d}x_B\, \mathrm{d}x_J\, Q_A(x_J,N_A;x_A)\, Q_B(x_B,N_B;x_J) \qquad \text{(II.18)}$$

Here $\tilde{Q}$ is a sort of single-chain partition function, and the exponential factor in eq II.17 that avoids "double-counting" the effects of the mean-field potentials arises naturally. [Note that the proportionality signs that we wrote before are now replaced by equality signs, since factors of π arising from doing Gaussian integrals and of $N!$ from distinguishability are present in both Z and Z_0 and cancel.] The average density of A monomers at a point x involves counting all the paths that pass through x (see Figure 3) and is given by

$$\rho_A(x) = \frac{N}{\tilde{Q}\rho_0 h}\int \mathrm{d}x_1\, \mathrm{d}x_2\, \mathrm{d}x_J \int_0^{N_A} \mathrm{d}s\, Q_A(x,s;x_1) \times Q_A(x,N_A-s;x_J)\, Q_B(x_J,N_B;x_2) \qquad \text{(II.19)}$$

and similarly for B monomers.

III. Factoring the Propagator

Let us consider the lamellar phase of a strongly segregated melt. Recall that the interfacial region between the nearly pure A and B microdomains is very narrow and sharp. Helfand[14,15] has shown that this leads to a separation of the interfacial and elastic energy contributions to the free energy, and we review his development here (although we shall use slightly different notation).

We consider a single repeat unit of width $h = h_A + h_B$ (see Figure 1) where $h_A = fh$ and $h_B = (1 - f)h$. From symmetry considerations, $Q_K(x,s;x_1)$ reflects at $x = h_A$, $-h_B$. We take the origin of our coordinate system at the dividing surface between the two domains where $\rho_A = \rho_B = 1/2$.[16]

Imagine a plane x_β that divides a pure A or B domain from the interface. On the scale of the interface $x_\beta \approx \infty$, but on the scale of the domain $x_\beta \approx 0$. This motivates us to write the full propagator as a product of a propagator for the pure domain and a propagator for the interface (see Figure 2) as follows

$$Q_K(x,s;x_1) = Q_K^b(x,s;x_1)\, q_K^I(x) q_K^I(x_1) \qquad \text{(III.1)}$$

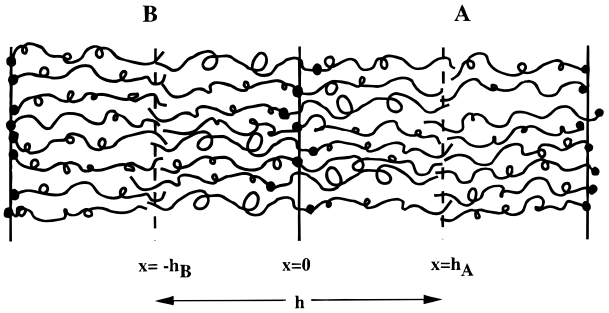

Figure 1. Unit cell for the lamellar microphase. Dotted lines indicate $K-K$ interfaces, while solid lines indicate $K-K'$ interfaces.

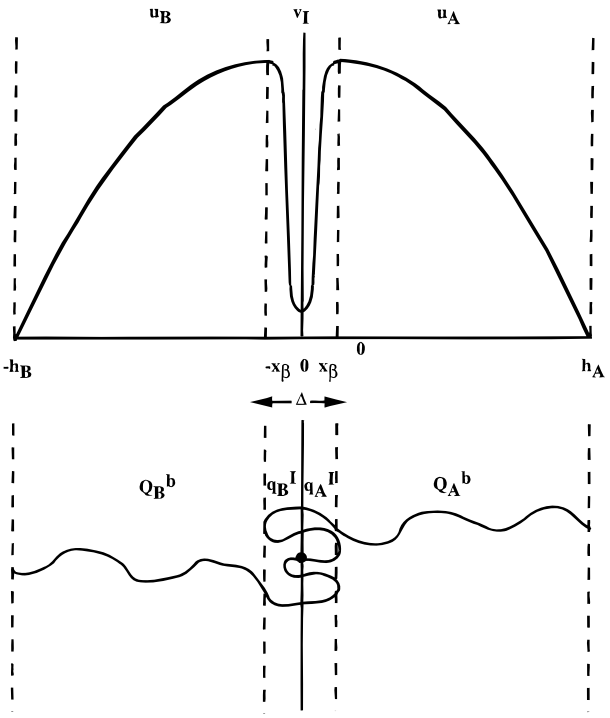

Figure 2. Schematic showing the region of validity of the homopolymer blend propagator (interfacial region) and the brush propagator (over the almost pure K domains) of eq III.1. Also shown are the corresponding pieces of the pressure field v^I and u_K.

where $q_K^I(x_2) \approx q_K^I(x_2, s) = \int \mathrm{d}x\, Q_K^I(x,s;x_2)$ is the propagator for a blend of A and B homopolymers and is almost unity over the domains except in the thin interfacial region. It satisfies the equation

$$0 = \frac{a^2}{6}\frac{\mathrm{d}^2 q_K^I}{\mathrm{d}x^2} - [v^I + \chi\rho_{K'}^I]q_K^I \qquad \text{(III.2)}$$

and $v^I(x)$ and $\rho_{K'}^I(x)$ are the external field and monomer density of the homopolymer blend solution. [See section IV for more details.]

$Q_K^b(x,s;x_\beta)$ is the propagator for a melt of homopolymers that are tethered at $x = 0$ (commonly known as a homopolymer "brush") since $Q_K^b(x,s;x_\beta) \approx Q_K^b(x,s;0)$. From the point of view of chains propagating over a K domain, x_β looks like a reflecting boundary condition due to the large repulsion from the K' domain:

$$0 \approx \left.\frac{\partial Q_K}{\partial x}\right|_{x_\beta} \approx \left.\frac{\partial Q_K^b}{\partial x}\right|_{x=0} \qquad \text{(III.3)}$$

[It is straightforward to see that $(\partial Q_K^b/\partial x)|_{x=h_k} = 0$ and that $Q_K^b(x,0;x_1) = \delta(x - x_1)$ from the boundary and initial conditions on the full propagator.]

To find what differential equation $Q_K^b(x,x_1;s)$ satisfies, we substitute eqs III.1 and III.2 into eq II.15

$$\frac{\partial Q_K^b}{\partial s} = \frac{a^2}{6}\frac{\partial^2 Q_K^b}{\partial x^2} + \frac{a^2}{3}\frac{\partial \log q_K^I}{\partial x}\frac{\partial Q_K^b}{\partial x} - [[v - v^I] + \chi[\rho_{K'} - \rho_{K'}^I]]Q_K^b \quad \text{(III.4)}$$

Notice that the second term on the right hand side vanishes because $q_K^I(x) \approx 1$ for $x \gg 0$, and $\partial Q_K^b/\partial x = 0$ for $x \approx 0$. Assuming that the monomer density profile through the interface closely approximates that for a homopolymer blend, $(\rho_{K'} - \rho_{K'}^I) \approx 0$, and we see that the factorization of eq III.1 is successful

$$\frac{\partial Q_K^b}{\partial s} = \frac{a^2}{6}\frac{\partial^2 Q_K^b}{\partial x^2} - u_K(x)Q_K^b \quad \text{(III.5)}$$

where

$$u(x) = v(x) - v^I(x) \quad \text{(III.6)}$$
$$= u_A(x) \qquad 0 \le x \le h_A$$
$$= u_B(x) \qquad -h_B \le x \le 0$$

This field is defined only within an additive constant which we fix by setting

$$\int_0^{h_K} dx\, u_K(x) = 0 \quad \text{(III.7)}$$

The pressure field $v(x)$ that maintains constant monomer density is then the sum of two pieces with two distinct characteristic length scales: a field that sucks monomers into the interfacial region against their enthalpic repulsion, and a field that pushes the chains out into the domains stretching the chains. In the coming sections, we shall give the specific form of these fields. For now we sketch these fields in Figure 2.

The factorization of the propagator can be used to separate the free energy into elastic and interfacial terms. Substituting eq III.1 into eq II.18 produces

$$\tilde{Q} \approx \frac{1}{h} a_J \tilde{Q}_A \tilde{Q}_B \quad \text{(III.8)}$$

where

$$a_J = \int_V dx_J\, q_A^I(x_J)\, q_B^I(x_J) \quad \text{(III.9)}$$

$$\tilde{Q}_K = \int_0^{h_K} dx_0\, Q_K^b(x_0,N_K;0) \quad \text{(III.10)}$$

Similarly, we may also write the monomer density as a product of the interfacial and brush factors

$$\rho_K(x) = \rho_K^b(x)\, \rho_K^I(x) \quad \text{(III.11)}$$

where

$$\rho_K^b(x) = \frac{\sigma}{\tilde{Q}_K \rho_0}\int_0^{N_K} ds\, Q_K^b(x,s;0)\int_0^{h_K} dx_0\, Q_K^b(x,N_K - s;x_0) \quad \text{(III.12)}$$

$$\rho_K^I(x) = [q_K^I(x)]^2 \quad \text{(III.13)}$$

where $\sigma = h/Na$ is the number of copolymer chains per unit volume. [In deriving eqs III.8 and III.12, we have assumed that $Q_K^b(x,s;x_J) \approx Q_K^b(x,s;0)$ since the A−B joints are localized in the interfacial region, and recall that $q_K^I(x) \approx 1$ for $x \gg 0$.] The equation set for $Q_K^b(x,s;x_1)$ is closed by determining $u_K(x)$ self-consistently so that $\rho_K^b(x) = 1$.

We use eq II.17 to write the free energy per chain (relative to the zero-field mixed state) as

$$F = F_{\text{interface}} + F_{\text{elastic}} \quad \text{(III.14)}$$

where

$$F_{\text{interface}} = \int_V dx\, \frac{Na^3\rho_0}{h}[-v^I(x) - \chi\rho_A\rho_B] - \ln\left[\frac{a_J}{h}\right] \quad \text{(III.15)}$$

$$F_{\text{elastic}} = -\ln\tilde{Q}_A - \ln\tilde{Q}_B \quad \text{(III.16)}$$

In summary, we have decomposed the problem of a diblock copolymer melt into two separate, well-studied problems: that of an infinite homopolymer blend and two homopolymer brushes, each of height h_K. [The validity of this narrow interface approximation was established in ref 14, by comparison of the free energy given by eqs III.15 and III.16 (using numerical solution of eq III.5), with the free energy calculated using the full numerical solution of eq II.15.]

IV. Interfacial Energy

The interface of a blend of high molecular weight homopolymers consists mostly of loops of monomers that weave back and forth across the interface. Chain ends are rare. In this limit, the propagator equation becomes independent of the monomer index s. [We may identify corrections to this limit by scaling s on N and x on $1/\chi^{1/2}$ (we shall see later that the interfacial width scales as $1/\chi^{1/2}$, so this is the relevant length scale). This produces an expansion parameter $1/(\chi N)$.]

The equation set for a homopolymer blend is[13]

$$0 = \frac{a^2}{6}\frac{\partial^2 q_A^I}{\partial x^2} - [\chi\rho_B^I + v^I]q_A^I \quad \text{(IV.1)}$$

$$0 = \frac{a^2}{6}\frac{\partial^2 q_B^I}{\partial x^2} - [\chi\rho_A^I + v^I]q_B^I \quad \text{(IV.2)}$$

[This form is identical to the ground-state equations for a quantum particle.] The solution to this equation set

is (see Appendix A for details)

$$\rho_A^I = \frac{\exp(2\sqrt{6\chi}x/a)}{1 + \exp(2\sqrt{6\chi}x/a)} \quad \text{(IV.3)}$$

$$\rho_B^I = \frac{1}{1 + \exp(2\sqrt{6\chi}x/a)} \quad \text{(IV.4)}$$

$$\nu^I = -3\chi\rho_A^I\,\rho_B^I \quad \text{(IV.5)}$$

Using the homopolymer blend density profile and potential in eq III.15 gives

$$F_{\text{interfacial}} = \frac{Na^3\rho_0}{h} 2\chi \int \mathrm{d}x\, \rho_A^I\,\rho_B^I - \ln(a_J/h)$$

$$= \sqrt{\frac{\chi}{6}}\frac{Na^4\rho_0}{h} - \ln\frac{\pi a}{2h\sqrt{6\chi}} \quad \text{(IV.6)}$$

where we have used the results

$$2\chi \int \mathrm{d}x\, \rho_A^I\,\rho_B^I = a\sqrt{\chi/6} \quad \text{(IV.7)}$$

$$a_J = \frac{\pi a}{2\sqrt{6\chi}} \quad \text{(IV.8)}$$

To make the physics of this expression for the interfacial free energy transparent, let us write it in the following way

$$F_{\text{interfacial}} = \sqrt{\frac{\chi}{6}}\frac{Na^4\rho_0}{h} + \ln\frac{h}{\Delta} + \ln\frac{4}{\pi} \quad \text{(IV.9)}$$

where Δ is the interfacial width which we have chosen to define by

$$\Delta = \left.\frac{\mathrm{d}x}{\mathrm{d}\rho_A}\right|_{x=0} = \frac{2a}{\sqrt{6\chi}} \quad \text{(IV.10)}$$

The first term of eq IV.9 is exactly the interfacial energy for a homopolymer blend. The second term arises from the homopolymers being connected. It represents the reduction in translational entropy to localize the joint to within Δ of the interface. In the reference state, the joints are free to be located throughout the entire layer thickness h. Hence we expect a confinement entropy per chain of precisely $\ln(h/\Delta)$. We will show in section VI that this term is subdominant in the limit $\chi N \to \infty$.

Semenov[17] has considered just such corrections in calculating interfacial widths for lamellar copolymers, using a different formalism (which produces good agreement with numerical self-consistent field calculations of the interfacial width by Matsen and Schick[18]). In Appendix B we show that his approach is entirely equivalent to Helfand's.

V. Elastic Energy

Having reviewed Helfand's results for separating the free energy and calculating the interfacial energy, we now turn to our derivation of the strongly-stretched brush theory. This will enable us to calculate the elastic energy of the copolymer domains. The elastic energy scales as $h^2/Na^2 \sim N^{1/3}$ since the strong-stretching domain period is known to scale with $aN^{2/3}$.[3] Thus for long chains a large pressure must exist to stretch the chains out over the height of the brush, which leads us to look for asymptotic solutions to equation III.5.

A. Asymptotic Expansion for the Propagator. The configuration of a polymer chain is analogous to the path of a quantum particle in an external field.[19] Indeed, equation III.5 has the same form as the Schrodinger equation, where $Q_K^b(x,s;x_1)$ is the probability density for a particle moving in an inverted potential $-u_K(x)$, with s playing the role of time. There exists an integral formulation for the path of a quantum particle[20] that is equivalent to the differential one. Exploiting this analogy, we can express the polymer propagator as a path integral

$$Q_K^b(x,s;x_1) = \int_{R(0)=x_1}^{R(s)=x} \mathrm{D}R\, \exp[-S_K\{R\}] \quad \text{(V.A.1)}$$

where $S_K\{R\}$ in quantum mechanical language is the action of a particle, given by

$$S_K\{R(s)\} = \int_0^s \mathrm{d}s' \left[\frac{3}{2a^2}\left(\frac{\mathrm{d}R}{\mathrm{d}s'}\right)^2 + u_K(R(s'))\right] \quad \text{(V.A.2)}$$

In the transition from quantum to classical mechanics, one identifies a single path that minimizes the action and thus represents the most significant contribution to the integral in equation V.A.2. This dominant path implies that the monomer position is no longer an independent variable but is instead specified by the monomer index. Thus, from now on, we shall denote the monomer position along the classical path by $x'(s';x_1,x,s)$. The arguments x_1, x, and s denote the beginning, end, and total number of steps, respectively, for this path. While x and s are used as arbitrary position and monomer independent variables at the end of a path, x' and s' are reserved as counters along this same path. When the path is N_K monomers long, we shall use x_0 to denote the chain end position, and x and s can then serve as counters along this path.

Expanding the action around this dominant path gives

$$S_K = S_{0,K}(x'(s')) + \frac{1}{2}\int \mathrm{d}s''\,\mathrm{d}s'''\,\delta R(s'')\,\delta R(s''') \times \left.\frac{\delta^2 S_K}{\delta x(s'')\,\delta x(s''')}\right|_{x'(s')} + \ldots \quad \text{(V.A.3)}$$

which enables us to write the propagator as

$$Q_K^b(x,s;x_1) \approx \exp[-(S_{0,K} + S_{1,K} + \ldots)] \quad \text{(V.A.4)}$$

This is in fact the WKB expansion (see for example ref 21) that is used to obtain global approximations to linear differential equations, when there is a small parameter multiplying the highest derivative in the equation. [In our case we see that scaling x by h_K and s by N_K produces $\delta = N_K a^2/h_K^2$ as the small parameter, which is vanishingly small in the limit of infinite N_K. Physically, the quantity $h_K/\sqrt{N_K}a$ relates how extended the brush chains are relative to their Gaussian coil configuration, and so is a measure of the degree of stretching of the brush. Then $S_{0,K}$ is a term of order $1/\delta$ and $S_{1,K}$ is a term of order unity. Details can be found in Appendix E.] Also, expanding the potential $u_K = u_{0,K}$

$+ u_{1,K}$ (where $u_{0,K}$ is $0(1/\delta)$ and $u_{1,K}$ is $O(1)$), and substituting eq V.A.4 into eq III.5 we get at zeroth-order

$$-\frac{\partial S_{0,K}(x,s;x_1)}{\partial s} = \frac{a^2}{6}\left(\frac{\partial S_{0,K}(x,s;x_1)}{\partial x}\right)^2 - u_{0,K}(x) \qquad \text{(V.A.5)}$$

This is the Hamilton−Jacobi equation (see for example ref 22) that describes the deterministic motion of a classical particle in an external field. The integral formulation for the classical action $S_{0,K}$ and its corresponding Euler−Lagrange equation for a chain segment that goes from $x_1 = x'(0)$ to $x = x'(s)$ is

$$S_{0,K}(x,s;x_1) = \int_0^s \mathrm{d}s' \left[\frac{3}{2a^2}\left(\frac{\mathrm{d}x'}{\mathrm{d}s'}\right)^2 + u_{0,K}(x'(s'))\right] \qquad \text{(V.A.6)}$$

$$\frac{3}{a^2}\frac{\partial^2 x'}{\partial s'^2} = \frac{\partial u_{0,K}}{\partial x'} \qquad \text{(V.A.7)}$$

Let us compute the variation in the action upon varying the end point of a path of s monomers such that $\delta x'(s) = x_2$ and $\delta x'(0) = 0$. Thus

$$\delta S_{0,K} = \int_0^s \mathrm{d}s' \left[\frac{3}{a^2}\frac{\mathrm{d}x'}{\mathrm{d}s'}\frac{\mathrm{d}\delta x'}{\mathrm{d}s'} + \frac{\mathrm{d}u}{\mathrm{d}x'}\delta x'\right] \qquad \text{(V.A.8)}$$

Integrating by parts in the first term and using the Euler−Lagrange equation (V.A.7), we see that

$$\frac{\partial S_{0,K}(x,s;x_1)}{\partial x} = \frac{3}{a^2}\frac{\mathrm{d}x'}{\mathrm{d}s'}\Big|_{s'=s} \qquad \text{(V.A.9)}$$

Since the classical action is just the free energy, eq V.A.9 has the physical interpretation that the virtual work of moving the end point of a chain segment is proportional to the tension $3(\mathrm{d}x/\mathrm{d}s)$ there.

At next order the propagator equation becomes

$$-\frac{\partial S_{1,K}(x,s;x_1)}{\partial s} = -\frac{a^2}{6}\frac{\partial^2 S_{0,K}(x,s;x_1)}{\partial x^2} + \frac{a^2}{3}\frac{\partial S_{0,K}(x,s;x_1)}{\partial x}\frac{\partial S_{1,K}(x,s;x_1)}{\partial x} - u_{1,K}(x) \qquad \text{(V.A.10)}$$

This is a first-order linear partial differential equation and so may be solved using the method of characteristics (see for example ref 23). The solution $S_{1,K}(x,s;x_1)$ is an integral surface (since it represents the integral of a partial differential equation); it may be constructed from a family of space curves in the surface known as characteristics. The characteristics are obtained by solving the following system of first-order ordinary differential equations

$$\frac{\mathrm{d}s}{1} = \frac{\mathrm{d}x}{\frac{a^2}{3}\frac{\partial S_{0,K}}{\partial x}} = \frac{\mathrm{d}S_{1,K}}{\frac{a^2}{6}\frac{\partial^2 S_{0,K}}{\partial x^2} + u_{1,K}(x)} \qquad \text{(V.A.11)}$$

where only one pair of equations is independent. Here, the characteristics are the perturbed chain paths in the field $u_{1,K}$ that propagate out from where the initial condition is prescribed. The first pair of equations shows that these paths are just the classical paths through eq V.A.9.

B. Determining the Potential at Lowest Order. In order to calculate $S_{0,K}$ and $S_{1,K}$, it is necessary to know $u_{0,K}$ and $u_{1,K}$. These constraint fields in turn must be determined by satisfying the incompressibility condition at each order. Upon examining eq III.12, we see that $Q^{\mathrm{b}}_K(x_0,N_K;0)$ can only vary by factors of unity in order to maintain constant density. Using eq V.A.4 for this propagator, we see that since $S_{0,K}(x_0,N_K;0)$ has a characteristic scale of $1/\delta$, it must be constant in order to satisfy eq III.12 at order $1/\delta$. Then, from eq V.A.9, the tension on the free end x_0 of a classical chain is zero.

Since all chains are N_K monomers long, we may write

$$N_K = \int_0^{N_K} \mathrm{d}s' = \int_0^{x_0} \frac{\mathrm{d}x'}{\mathrm{d}x'/\mathrm{d}s'} \qquad \text{(V.B.1)}$$

Integrating the Euler−Lagrange equation once gives

$$\frac{3}{2a^2}\left(\frac{\mathrm{d}x'}{\mathrm{d}s'}\right)^2 = u_{0,K} - u_f \qquad \text{(V.B.2)}$$

where $u_f = u_{0,K}(x_0)$ and we have used $\mathrm{d}x'/\mathrm{d}s'|_{x_0} = 0$. Substituting eq V.B.2 into eq V.B.1 and changing variables to $u_{0,K}$ gives

$$N_K = \int_{A_K}^{u_f} \mathrm{d}u_{0,K}\frac{\mathrm{d}x'}{\mathrm{d}u_{0,K}}\sqrt{\frac{3}{2a^2(u_{0,K}-u_f)}} \qquad \text{(V.B.3)}$$

where we have defined $A_K = u_{0,K}(x = 0)$. This is an integral equation for $\mathrm{d}x'/\mathrm{d}u_{0,K}$, which may be inverted using the method of Appendix C (where eq V.C.16 is solved as an example) to give

$$u_{0,K}(x) = A_K - B_K x^2 \qquad \text{(V.B.4)}$$

where $B_K = 3\pi/8N_K^2a^2$. The overall level of the potential is fixed by requiring that $\int_0^{hK} \mathrm{d}x\, u_{0,K} = 0$, which results in $A_K = B_K h_K^2/3$. As we shall see in the next section, such a parabolic potential profile does indeed produce a constant classical action for a walk of N_K monomers and therefore is the correct potential at this level of approximation.

The traditional method[4] of deriving the classical parabolic potential is to recognize that a chain tethered at $x = 0$ with its free end at x_0 is analogous to a classical particle that starts from rest at x_0 and falls in "time" N_K to the grafting surface. Since the time to fall to the surface is the same for all x_0, the particle is a harmonic oscillator of mass $3/a^2$ and "spring constant" $(2B_K)^{1/2} = 2\pi/\tau_K$, where the path of each particle is one-quarter cycle $\tau_K = 4N_K$.

C. Finding $u_{1,K}$ from Satisfying the Incompressibility Constraint. We shall determine $u_{1,K}(x)$ by directly solving eq III.12 such that $\rho^{\mathrm{b}}_K(x) = 1$. In order to evaluate the brush density we need to evaluate two types of terms, $\tilde{Q}^{\mathrm{b}}_K(x,s) = \int_0^{hK} \mathrm{d}x_0\ Q^{\mathrm{b}}_K(x,s;x_0)$ and $Q^{\mathrm{b}}_K(x,s;0)$. We shall do this by using the WKB approximation we have described above.

Let us consider a chain segment that propagates from x_1 to x_2 in s monomers. Solving eq V.A.7 gives us the classical path between these two points

$$x'(s';x_1,x_2,s) = \frac{x_2 - x_1\cos\omega_K s}{\sin\omega_K s}\sin\omega_K s' + x_1\cos\omega_K s' \qquad \text{(V.C.1)}$$

where $\omega_K = \pi/2N_K$. Substituting this path into eq V.A.6

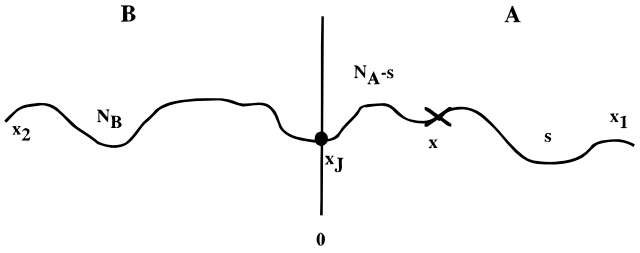

Figure 3. Typical chain that contributes to the monomer density given by eq II.19.

gives us the classical action

$$S_{0,K}(x_2,s;x_1) = \frac{3\omega_K}{2}\left[(x_1^2 + x_2^2)\cot \omega_K s - \frac{2x_1x_2}{\sin \omega_K s}\right] + \frac{B_K h_K^2}{3}s \quad \text{(V.C.2)}$$

which is symmetric under interchange of x_1 and x_2 as required.

We then want to evaluate $S_{1,K}(x_2,s;x_1)$ by solving eq V.A.11, which gives us

$$S_{1,K}(x_2,s;x_1) = \frac{1}{2}\ln \sin \omega_K s + \int_0^s ds'\, u_{1,K}(x'(s';x_1,x_2,s)) + a_1 \quad \text{(V.C.3)}$$

where we determine the constant $a_1 = \log(3\omega_K/2\pi a^2)^{1/2}$ by satisfying the intial condition $Q_K^b(x_2,0;x_1) = \delta(x_1 - x_2)$.

Thus the propagator is written

$$Q_K^b(x_2,s;x_1) = \left(\frac{3\omega_K}{2\pi a^2 \sin \omega_K s}\right)^{1/2} \times \exp[-\int_0^s ds'\, u_{1,K}(x'(s';x_1,x_2,s))] \exp\left[-\frac{3\omega_K}{2a^2}\left[(x_1^2 + x_2^2)\cot \omega_K s - \frac{2x_1x_2}{\sin \omega_K s}\right] - \frac{B_K h_K^2}{3}s\right] \quad \text{(V.C.4)}$$

We evaluate $\bar{Q}_K^b(x,s)$ by doing the integral over x_0 by saddle-points, where the more-slowly varying factor of $\exp[-S_{1,K}]$ may be taken outside the integral, enabling us to do the remaining Gaussian integral involving $S_{0,K}$

$$\bar{Q}_K^b(x,s) = \exp[-S_{1,K}(x,s;x_0^*)]\left(\frac{2\pi}{3\omega_K \cot \omega_K s}\right)^{1/2} \times \exp\left[\frac{3\omega_K}{2a^2}x^2 \tan \omega_K s - \frac{B_K h_K^2}{3}s\right] \quad \text{(V.C.5)}$$

The saddle-point value $x_0^*(x,s)$ is given by

$$x = x_0^*(x,s)\cos \omega_K s \quad \text{(V.C.6)}$$

which specifies a most-likely end point x_0 corresponding to a segment that has reached x in s steps. Figure 5 shows a "brush path" that starts at the wall and ends at x_0^* in N_K monomers.

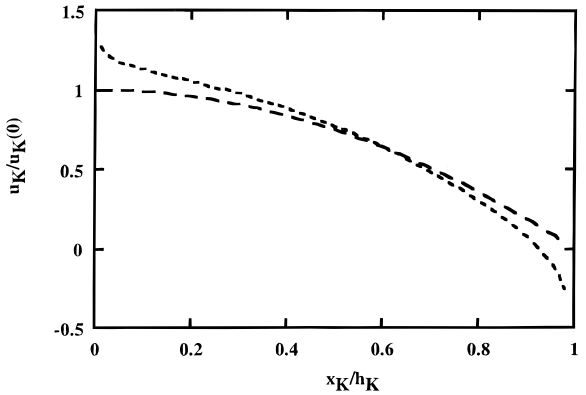

Figure 4. Parabolic brush pressure field at lowest order, $u_{0,K}$ (wide dashed line). The leading correction $u_{1,K}$ (narrow dashed line) diverges at the origin and tip of the brush. The plot here is for a brush with $h_K/\sqrt{N_K a} = 3$.

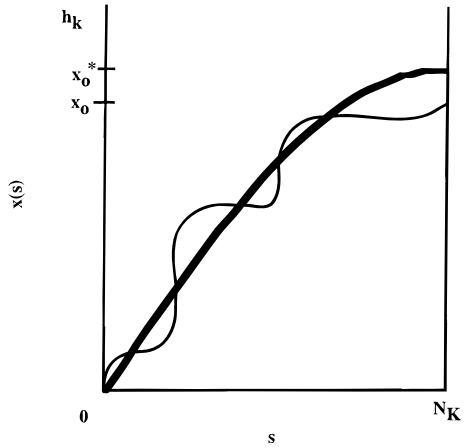

Figure 5. Classical path (dark line) that represents the dominant contribution from a chain N_K monomers long to the brush density given by eq III.12. This path has the chain free end at x_0^*. We also show (light lines) other possible classical paths corresponding to less likely positions of the chain end.

We then evaluate $S_{1,K}(x,s;x_0^*)$ using eq V.C.3 and the saddle-point path to give

$$\bar{Q}_K^b(x,s) = \left(\frac{1}{\cos \omega_K s}\right)^{1/2} \times \exp[-\int_0^s ds'\, u_{1,K}(x'(s';x,x_0^*,s))] \times \exp\left[\frac{3\omega_K}{2a^2}x^2 \tan \omega_K s - \frac{B_K h_K^2}{3}s\right] \quad \text{(V.C.7)}$$

For the second type of term, $Q_K^b(x,s;0)$, we must consider a chain path that goes from 0 to x in s steps. The propagator for such a path using eq V.C.4

$$Q_K^b(x,s;0) = \left(\frac{3\omega_K}{2\pi a^2 \sin \omega_K s}\right)^{1/2} \times \exp[-\int_0^s ds'\, u_{1,K}(x'(s';0,x,s))] \times \exp\left[-\frac{3\omega_K}{2}x^2 \cot \omega_K s - \frac{B_K h_K^2}{3}s\right] \quad \text{(V.C.8)}$$

which corresponds to a path (from eq V.C.1)

$$x'(s';0,x,s) = \frac{x}{\sin \omega_K s}\sin \omega_K s' \quad \text{(V.C.9)}$$

We may now calculate the brush density using eqs V.C.7 and V.C.8 in eq III.12. The exponential factors from the classical action in the numerator combine to give $\exp[-B_K h_K^2 N_K/3]$, which in turn cancels an identical factor in the denominator. This gives

$$\rho_K^b(x) = \frac{\sigma}{\int_0^{h_K} dx_0 \exp[-\int_0^{N_K} ds'\, u_{1,K}(x'(s';0,x_0,N_K))]} \times \int_0^{N_K} ds \{\exp[-\int_0^{s} ds'\, u_{1,K}(x'(s';0,x,s))] \times \exp[-\int_s^{N_K} ds'\, u_{1,K}(x'(s';x,x_0^*,N_K-s))]\}/\sin \omega_K s \quad \text{(V.C.10)}$$

Let us define an (as yet) unknown function $\epsilon_K(x_0)$

$$\epsilon_K(x_0) = \exp\left[-\int_0^{x_0} dx \frac{ds}{dx} u_{1,K}(x)\right] \quad \text{(V.C.11)}$$

such that the integrals over $u_{1,K}$ in the numerator (from the $S_{1,K}$ terms) may be combined to give $\epsilon_K(x_0^*(x,s))$.

Note that the combination of these integrals into one implies that the paths from the factors $Q_K^b(x,s;0)$ and $\bar{Q}_K^b(x, N_K - s)$ are the same. This "brush path" for a walk of N_K steps from the wall at $x = 0$ to an end position at x_0^* represents the dominant contribution to the brush density from all possible classical paths and is described by

$$x(s) = x_0^* \sin \omega_K s \quad \text{(V.C.12)}$$

We may show that this is true by replacing s and x with N_K and x_0^*, respectively, in eq V.C.9 and by replacing s with $(N_K - s)$ in eq V.C.6. Equation V.C.12 is then the position of the sth monomer along a chain grafted at $x = 0$ with its end at x_0^*. From now on, since we shall be considering walks of N_K monomers, we shall drop s' and use s as our index along the chain.

If we consider the probability for a walk of N_K steps to the grafting surface, $Q_K^b(x_0,N_K;0)$, we see that the classical action is independent of the chain end position (i.e. $S_{0,K}(x_0,N_K;0) = \exp[-B_K h_K^2 N_K/3]$) and that $\epsilon_K(x_0)$ is in fact the distribution function for chain ends within the brush.

The density may thus be written as

$$\rho_K^b(x) = \frac{\sigma}{\int_0^{h_K} dx_0\, \epsilon_K(x_0)} \int_0^{N_K} ds \frac{\epsilon_K(x_0^*(x,s))}{\sin \omega_K s} \quad \text{(V.C.13)}$$

Let us now change the integral over ds to an integral over dx_0^*, and recognize that differentiating eq V.C.12 with respect to s, holding x fixed, and letting x_0^* and s vary gives us

$$0 = \frac{dx_0^*}{ds} \sin \omega_K s + x_0^* \omega_K \cos \omega_K s \quad \text{(V.C.14)}$$

Rearranging gives

$$\frac{ds}{dx_0^*} = -\frac{\sin \omega_K s}{dx/ds} \quad \text{(V.C.15)}$$

where dx/ds is the differential of eq V.C.12 for a chain with its end held fixed at x_0^*. This allows us to write the density as

$$\rho_K^b(x) = \frac{\sigma}{\int_0^{h_K} dx_0\, \epsilon_K(x_0)} \int_x^{h_K} dx_0^* \left|\left|\frac{ds}{dx}\right|\right|_{x \to x^* 0} \epsilon_K(x_0^*) \quad \text{(V.C.16)}$$

[The subscript indicates that a brush path from x to x_0^* must be used.] Note that the lower limit on the integral over x_0^* is x. This is because the classical path cannot turn back on itself so chain paths that pass through x must have their end points beyond x.

Setting $\rho_K^b(x) = 1$ in eq V.C.16 gives us an integral equation for $\epsilon(x_0)$ which may be solved (see Appendix C) to give

$$\epsilon_K(x_0) = \frac{1}{2} \frac{x_0}{(h_K^2 - x_0^2)^{1/2}} \quad \text{(V.C.17)}$$

where we have chosen to normalize $\int_0^{hK} dx_0\, \epsilon_K(x_0) = h_K/2$. [Our choice of normalization assures $\int dx\, u_{1,K}(x) = 0$ (see below) but is by no means unique.] A plot of the end density is shown in Figure 6.

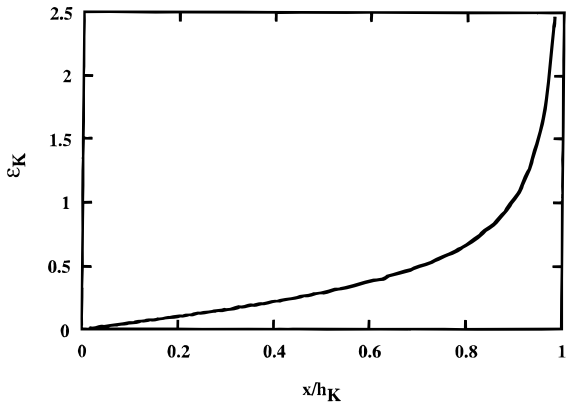

Figure 6. Distribution function $\epsilon(x)$ of free ends in the brush at this level of approximation, which is zero at the origin and diverges at $x = h_K$. At next order chains are able to penetrate into the next brush and the end density peaks around the brush tip and goes to zero beyond it.

Having determined $\epsilon_K(x_0)$, we can now solve eq V.C.11 for $u_{1,K}(x)$ (see Appendix D)

$$-N_K u_{1,K}(x) = \ln \frac{x}{h_K} + \sqrt{\frac{x^2}{h_K^2 - x^2}} \arctan \sqrt{\frac{x^2}{h_K^2 - x^2}} \quad \text{(V.C.18)}$$

[Note that the perturbing potential as previously calculated in ref 24 contains typographical errors.] We have the unphysical result that the perturbing potential diverges at the tip of the brush in order to force the end density to zero there (see Figure 4). In reality the chains extend beyond h_K into the next domain and $\epsilon(x)$ peaks at the start of this penetration zone and decays to zero at the end of it. These corrections to the perturbing potential calculated above, however, only enter at the next order and we will have more to say about them in section VII.

The perturbing potential is also singular at the grafting surface, although the divergence is logarithmic and thus much weaker (also see section VII).

D. Asymptotic Elastic Free Energy. We use eq V.C.8 to evaluate $\tilde{Q}_K$ for each domain

$$\tilde{Q}_K = \frac{\sqrt{3}}{4}\frac{h_K}{a\sqrt{N_K}}\exp\left[-\frac{\pi^2}{8}\frac{{h_K}^2}{a^2 N_K}\right] \qquad \text{(V.D.1)}$$

The elastic energy per chain is then

$$F_{\text{elastic}} = \frac{c_0 h^2}{Na^2} + \ln\left(c_1\frac{Na^2}{h^2}\right) \qquad \text{(V.D.2)}$$

where $c_0 = \pi^2/8$ and $c_1 = 16/(3\sqrt{f(1-f)})$. The first term arises from the classical description of the chain and is of the same magnitude as the homopolymer interfacial free energy. The second term comes from entropic fluctuations about the classical path which contributes constant logarithmic terms to the free energy at the same order as the joint localization energy in our calculation of the interfacial free energy. These corrections therefore represent finite-N corrections[25] to the asymptotic free energy. Physically, they represent the entropy gain for the wandering of the free chain end over the brush. By contrast in the reference state the free end is typically found within the radius of gyration of the joint position. Since there are two free ends per chain, we thus expect an entropic contribution per chain of $2\ln(\sqrt{N_K}a/h_K)$. [See also the discussion following eq IV.9.]

VI. Expansion of the Free Energy

We are now in a position to organize our results as an expansion of the free energy in a small parameter ϵ. The free energy per chain from eq IV.6 and V.D.2 is

$$F = \frac{c_0 h^2}{Na^2} + (\rho_0 a^3)\sqrt{\frac{\chi}{6}}\frac{Na}{h} + \left[\frac{2\sqrt{6\chi}c_1}{\pi}\frac{Na}{h}\right] \qquad \text{(VI.1)}$$

Note that the corrections from the elastic energy are negative while those from the interfacial energy are positive. However, there are two chain ends but only one joint per chain, so that overall the corrections increase the asymptotic free energy.

Let us scale the domain period so that $\tilde{h} = h/(a\chi^{1/6}N^{2/3})$ and identify the small parameter to be $\epsilon = 1/(\chi N)^{1/3}$. Then

$$\epsilon F = \tilde{F} = c_0\tilde{h}^2 + \frac{\rho_0 a^3}{\sqrt{6}\tilde{h}} - \epsilon\ln\epsilon + \epsilon\ln\left[\frac{c_1 2\sqrt{6}}{\pi\tilde{h}}\right] \qquad \text{(VI.2)}$$

Also expanding the period $\tilde{h} = \tilde{h}_0 + \epsilon\tilde{h}_1$ and minimizing $\tilde{F}$ with respect to $\tilde{h}$ gives

$$\tilde{h}_0 = \left(\frac{\rho_0 a^3}{2c_0\sqrt{6}}\right)^{1/3} \qquad \text{(VI.3)}$$

$$\tilde{h}_1 = \frac{1}{\tilde{h}_0[2c_0 + (2\rho_0 a^3/\sqrt{6}{\tilde{h}_0}^3)]} \qquad \text{(VI.4)}$$

The logarithmic corrections to the free energy do not affect the period since they are independent of $\tilde{h}$. Substituting the minimized $\tilde{h}$ into eq VI.2 gives the minimized free energy $\tilde{F} = \tilde{F}_0 - \epsilon\ln\epsilon + \epsilon\tilde{F}_1$ where

$$\tilde{F}_0 = c_0{\tilde{h}_0}^2 + \frac{1}{\sqrt{6}\tilde{h}_0}(\rho_0 a^3)^{2/3} \qquad \text{(VI.5)}$$

$$\tilde{F}_1 = \ln\left[\frac{2\sqrt{6}c_1}{\pi\tilde{h}_0}\right] - \frac{\tilde{h}_1\rho_0 a^3}{\sqrt{6}{\tilde{h}_0}^2} + 2c_0\tilde{h}_0\tilde{h}_1 \qquad \text{(VI.6)}$$

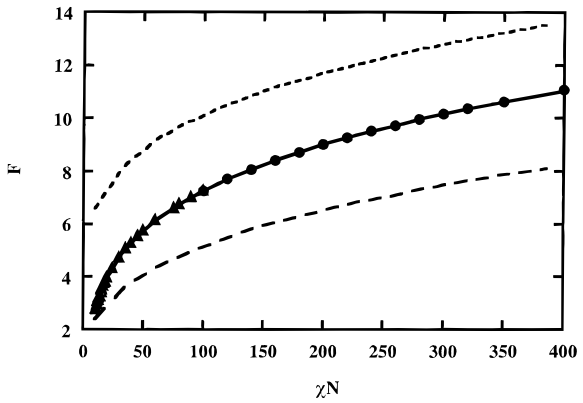

Figure 7. Asymptotic free energy (wide dashed line) lies below the numerical data (solid line, circles indicate data from ref 26, triangles indicate data from ref 27). Adding the leading corrections (narrow dashed line) puts the free energy above the numerical data. Here $f = 0.5$.

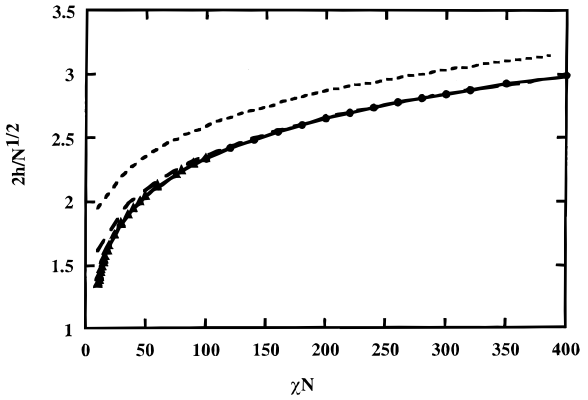

Figure 8. Asymptotic domain period (wide dashed line) is in excellent agreement with the numerical data (solid line, circles indicate data from ref 26, triangles indicate data from ref 27). Adding the leading corrections worsens agreement considerably (narrow dashed line).

We plot in Figures 7 and 8 the unscaled asymptotic free energy and domain period compared to numerical data from Matsen[26] and Whitmore[27] (where we have set the dimensionless quantity $\rho_0 a^3 = 1$). These are numerical solutions of eq II.15 and so provide a direct test of the range over which our approximations are valid. [We recall that the reference state is the mixed homogeneous melt with $\chi = 0$, so that at the ordering transition at $\chi N = 10.5$ for $f = 0.5$[2] the free energy is not zero.] We see that while the asymptotic free energy is several $k_B T$ less from the numerical results, the asymptotic domain period is in excellent agreement. We note that the numerical results do in fact show a larger period at smaller χN.

Upon adding the leading corrections to the free energy we see that we increase the free energy to a few $k_B T$ above the numerical data. This is at the expense of agreement with the domain radius, which now appears to increase with χN since the correction term is positive and is opposite to the trend we were trying to predict.

VII. Higher Order Corrections

Physically, the most obvious next-order corrections are due to the penetration of opposing brushes. At the order of the calculations above, these brushes cannot penetrate each other. However, the potential $u_{0,K}$ is internally inconsistent, since over a small region ξ at the foot of the brush, the potential is low enough that the chain can relax back to a random walk. Here, $u_{0,K}(h_K - \xi) \sim (h\xi/N_K{}^2a^2)$ and a walk of k monomers can only penetrate a distance $\xi \sim k^{1/2}a$ since a larger distance would cause substantial stretching. Penetration is allowed for $u_{0,K}(h_K - \xi)k \leq 1$ (balancing the gain in translational entropy against the energy of penetration) so monomer lengths of order $k^{3/2} \leq N_K{}^2a^2/h_K$ can penetrate over a characteristic length such that $(\xi/h_K) \sim (\sqrt{N_K}a/h_K)^{4/3}$.[28]

The width of this penetration zone also marks the place where the parabolic potential breaks down. At the edge of the penetration zone, $u_{1,K}(h_K - \xi) \sim (1/N_K)\sqrt{h_K/\xi}$. Considering where $u_{1,K}$ is the same scale as $u_{0,K}$ also gives an estimate for ξ that is the same as above. [Estimating where $u_{1,K} \approx u_{0,K}$ at the grafting surface leads to a region of width $\zeta/h \sim \exp[-h_K{}^2/N_Ka^2]$, so the corrections due to this region are exponentially small.] Consequently the perturbing potential and the end density themselves are modified through these higher-order corrections, and the unphysical divergences evaporate.

The end density has a square root singularity at the tip of the brush (see eq V.C.17), so the number of ends in the penetration region scales as $(\xi/h_K)^{1/2}$. Each end in the zone perturbs the free energy by k_BT, so corrections to the free energy per chain scale as $(\xi/h_K)^{1/2} \sim 1/(\chi N)^{1/9}$ (since $h_K \sim \chi^{1/6}aN_K{}^{2/3}$). These correspond to terms of order $\chi N^{-4/9}$ in the free energy expansion and are not much smaller than the leading order terms (at $O(\chi N^{-1/3})$) we have calculated for the range of χN considered in Figures 7 and 8.

Recently, Orland and Schick[29] have calculated corrections to the classical end density for a single solvent brush. They use a classical path composed of a sine and cosine in an integral equation for the brush density and obtain reasonable agreement with numerical data for the density of chain ends. However, their method is somewhat heuristic since the actual potential in the "foot" of the brush (at this order) is clearly not parabolic, so that the classical path must take a different functional form than they have proposed. Indeed, their results for the density of free ends far from the classical brush edge do not agree with known asymptotic results.[30]

In a subsequent paper, Netz and Schick[31] derive the classical free energy for a solvent brush, by considering only classical chain paths and extremizing the single chain free energy with respect to the brush density and end distribution. For nonzero $\delta = N_Ka^2/h_K{}^2$ ($1/\beta$ in the terminology of ref 31), they find an entropic contribution to the single chain free energy that is δ times smaller than the classical free energy. They extremize this free energy at finite β to obtain corrections to the classical brush density, end distribution and find non-zero stretching at the free chain end. As we have systematically shown in this paper, such corrections must also include fluctuations of the path itself about the classical path in order to be consistent at the right order in $(1/\delta)$.

VIII. Conclusions

In summary, we have derived the strong-stretching approximation from the full partition function for strongly-segregated diblock copolymer melts. The approximation is exact in the limit $\chi N \to \infty$. We calculate the leading order corrections to this theory by transcribing previous results of Helfand for the interfacial free energy and using a WKB expansion to calculate the elastic free energy.

These corrections scale as $\log \chi N$ and arise from the wandering of the chain ends over the domain and the localization of junction points in the interfacial region. These represent an entropy gain and an entropy loss, repectively, and since there are two chain ends for every joint, the corrections are positive overall. The asymptotic free energy is a few k_BT below the numerical data, while the asymptotic domain period is in good agreement with numerical data. The leading corrections shift the free energy to a few k_BT above the numerical data, and cause the domain period to show an apparent lower scaling exponent. Experimental and numerical evidence show an opposite trend for the domain period, that the domain period shows a higher apparent scaling exponent.

The next order corrections arising from interpenetration between like domains scale as $(\chi N)^{-1/9}$, and are thus large enough to qualitatively change the results above at intermediate χN. If these corrections were negative in sign, both the free energy and the domain period would be brought into better agreement with the numerical data.

It is important to keep in mind, however, that the expansion is an asymptotic one and that asymptotics tells us that generating corrections to an asymptotic limit only improves the approximate result up to a certain point before it diverges from the exact solution. This may well be the case here. Nevertheless, we feel that it is significant to have identified the shortcomings of such a widely accepted theory in a systematic way.

We have carried out our analysis for a lamellar phase for simplicity. In principle, this can be extended to other geometries but will require more elaborate computation due to the dead zones in the domain, which exclude chain ends in the cylindrical and spherical geometries.[32,33]

Acknowledgment. This work was supported primarily by the MRSEC program of the National Science Foundation under Award Number DMR-9400362. We thank M. Matsen and M. Whitmore for kindly supplying us with their numerical data.

Appendix A: Interfacial Profile for a Homopolymer Blend

The coupled ground-state equations for a homopolymer blend are

$$0 = \frac{a^2}{6}\frac{\mathrm{d}^2 q_{\mathrm{A}}^{\mathrm{I}}}{\mathrm{d}x^2} - [\chi\rho_{\mathrm{B}} + v^{\mathrm{I}}]q_{\mathrm{A}}^{\mathrm{I}} \qquad \text{(A.1)}$$

$$0 = \frac{a^2}{6}\frac{\mathrm{d}^2 q_{\mathrm{B}}^{\mathrm{I}}}{\mathrm{d}x^2} - [\chi\rho_{\mathrm{A}} + v^{\mathrm{I}}]q_{\mathrm{B}}^{\mathrm{I}} \qquad \text{(A.2)}$$

Let us scale

$$\bar{x} = \frac{\sqrt{6\chi}x}{a} \tag{A.3}$$

$$\bar{v}^{\mathrm{I}} = \frac{v^{\mathrm{I}}}{\chi} \tag{A.4}$$

Multiplying eq A.1 by $q_{\mathrm{B}}^{\mathrm{I}}$, and eq A.2 by $q_{\mathrm{A}}^{\mathrm{I}}$ and subtracting them eliminates v^{I}. We can then use the ground-state relation $q_K^{\mathrm{I}} = \sqrt{\rho_K^{\mathrm{I}}}$ and the constraint $\rho_{\mathrm{A}}^{\mathrm{I}} + \rho_{\mathrm{B}}^{\mathrm{I}} = 1$ to give an ordinary differential equation for

$$0 = \frac{1}{2}\frac{1}{\rho_{\mathrm{A}}^{\mathrm{I}}(1-\rho_{\mathrm{A}}^{\mathrm{I}})}\frac{\mathrm{d}^2\rho_{\mathrm{A}}^{\mathrm{I}}}{\mathrm{d}\bar{x}^2} + \frac{1}{4}\frac{2\rho_{\mathrm{A}}^{\mathrm{I}} - 1}{\rho_{\mathrm{A}}^{\mathrm{I}\,2}(1-\rho_{\mathrm{A}}^{\mathrm{I}})^2}\left(\frac{\mathrm{d}\rho_{\mathrm{A}}^{\mathrm{I}}}{\mathrm{d}\bar{x}}\right)^2 + (2\rho_{\mathrm{A}}^{\mathrm{I}} - 1) \tag{A.5}$$

We can reduce the order of this equation by one by using the substitution $p = \mathrm{d}\rho_{\mathrm{A}}^{\mathrm{I}}/\mathrm{d}\bar{x}$, so that

$$\frac{\mathrm{d}^2\rho_{\mathrm{A}}^{\mathrm{I}}}{\mathrm{d}x^2} = \frac{\mathrm{d}p}{\mathrm{d}x} = \frac{\mathrm{d}p}{\mathrm{d}\rho_{\mathrm{A}}^{\mathrm{I}}}\frac{\mathrm{d}\rho_{\mathrm{A}}^{\mathrm{I}}}{\mathrm{d}x} = p\frac{\mathrm{d}p}{\mathrm{d}x} \tag{A.6}$$

Equation A.5 may then be solved to give

$$\frac{\mathrm{d}\rho_{\mathrm{A}}^{\mathrm{I}}}{\mathrm{d}\bar{x}} = 2\rho_{\mathrm{A}}^{\mathrm{I}}(1-\rho_{\mathrm{A}}^{\mathrm{I}}) \tag{A.7}$$

where we have used the boundary condition $\mathrm{d}\rho_{\mathrm{A}}^{\mathrm{I}}/\mathrm{d}\bar{x} = 0$ at $\rho_{\mathrm{A}}^{\mathrm{I}} = 1$ and $\rho_{\mathrm{A}}^{\mathrm{I}} = 0$.

Solving eq A.7 results in eqs IV.3 and IV.5 for the monomer density profile through the interface. These densities may be used in eq A.1 to calculate the interfacial pressure field given by eq IV.5.

Appendix B. Semenov's Corrections to the Asymptotic Interfacial Energy

Let us start with the integral given by eq III.9, which we rewrite as

$$a_{\mathrm{J}} = \frac{1}{h}\int_V \mathrm{d}x_{\mathrm{J}}\, \exp[-W(x_{\mathrm{J}})] \tag{B.1}$$

which is the partition function for a dilute gas of junction points in a potential $-W = \log(\rho_{\mathrm{A}}^{\mathrm{I}}\,\rho_{\mathrm{B}}^{\mathrm{I}})^{1/2}$.

We want to convert the integral over the position of junction points to one over the density of junction points so we write

$$a_{\mathrm{J}} = \frac{1}{h}\int \mathrm{D}\rho_{\mathrm{J}} \int \mathrm{d}x_{\mathrm{J}}\, \delta(\rho_{\mathrm{J}} - \hat{\rho}_{\mathrm{J}})\, \exp[-W(x_{\mathrm{J}})] \tag{B.2}$$

where $\rho_{\mathrm{J}}(x)$ is the junction point density for a single chain and $\hat{\rho}_{\mathrm{J}}(x) = \delta(x - x_{\mathrm{J}})$. Exponentiating the δ-function

$$a_{\mathrm{J}} = \frac{1}{h}\mathrm{D}\rho_{\mathrm{J}} \int \mathrm{d}x_{\mathrm{J}} \int \mathrm{D}\omega\, \exp[-\int \mathrm{d}x_{\mathrm{J}}\, \omega(\rho_{\mathrm{J}} - \hat{\rho}_{\mathrm{J}})] \times \exp[-W(x_{\mathrm{J}})] \tag{B.3}$$

We want to evaluate the integral over ω by saddle-points so we write eq B.3 as

$$a_{\mathrm{J}} = \frac{1}{h}\int \mathrm{D}\rho_{\mathrm{J}} \int \mathrm{D}\omega\, \exp[-\int \mathrm{d}x_{\mathrm{J}}\, \omega\rho_{\mathrm{J}} + \log(\int \mathrm{d}x_{\mathrm{J}}\, \exp[\omega(x_{\mathrm{J}}) - W(x_{\mathrm{J}})])] \tag{B.4}$$

The saddle-point value of $\omega(x_{\mathrm{J}})$ is given by

$$\omega(x_{\mathrm{J}}) = \log \rho_{\mathrm{J}} - \log C + W(x_{\mathrm{J}}) \tag{B.5}$$

where C is a constant we shall determine. Substituting eq B.5 into eq B.4 gives

$$a_{\mathrm{J}} = \frac{1}{h}\int \mathrm{D}\rho_{\mathrm{J}}\, \exp[\int x_{\mathrm{J}}(-\rho_{\mathrm{J}} \log \rho_{\mathrm{J}} - W\rho_{\mathrm{J}}) + \log C(\int \mathrm{d}x_{\mathrm{J}}\, \rho_{\mathrm{J}} - 1)] \tag{B.6}$$

Now doing the integral over ρ_{J} by saddle-points gives $\rho_{\mathrm{J}} = C(\rho_{\mathrm{A}}\rho_{\mathrm{B}})^{1/2}$. We set $\int \mathrm{d}x_{\mathrm{J}}\, \rho_{\mathrm{J}} = 1$ so C must equal $4/(\Delta\pi)$. Then

$$\ln(a_{\mathrm{J}}/h) = \int \mathrm{d}x_{\mathrm{J}}\, [\rho_{\mathrm{J}} \log \rho_{\mathrm{J}} + W\rho_{\mathrm{J}}] \tag{B.7}$$

which is equation 3.4 of ref 17. [Note that unlike Semenov, we do not find any additive constants for eq B.7.] Performing the integration in eq B.7 using the junction point density calculated above gives eq IV.8.

Appendix C. Solving for End Density

We wish to solve the integral equation

$$\frac{\sigma}{\int_0^{h_K}\epsilon_K(x_0)}\int_x^{h_K}\mathrm{d}x_0\,\frac{2N_K}{\pi}\frac{\epsilon_K(x_0)}{\sqrt{x_0^2 - x^2}} = 1 \tag{C.1}$$

Let us change variables to $t_0 = (x_0/h_K)^2$

$$\int_t^1 \mathrm{d}t_0\,\frac{f(t_0)}{\sqrt{(t_0 - t)}} = \frac{\pi}{2} \tag{C.2}$$

where we have defined $t = (x/h_K)^2$ and $f(t_0) = \epsilon_K(t_0)/\sqrt{t_0}$. We would like to cast this integral into the form of a convolution so we change variables again to $y_0 = 1 - t_0$

$$\int_0^y \mathrm{d}y_0\,\frac{f(y_0)}{\sqrt{(y - y_0)}} = \frac{\pi}{2} \tag{C.3}$$

where $y = 1 - t$. Let us now recall the convolution theorem for Laplace transforms

$$L[\int_0^t \mathrm{d}\tau\, y_1(t-\tau)\, y_2(\tau)] = L[y_1(t)]\, L[y_2(t)] \tag{C.4}$$

where $L[f(t)](s) = \int_0^\infty \mathrm{d}t\, \mathrm{e}^{-st}\, f(t)$. Then we want to Laplace transform both sides of eq C.3 so that

$$L[f(y_0)] = \frac{1}{2}\sqrt{\frac{\pi}{s}} \tag{C.5}$$

Transforming back gives us

$$f(y_0) = \frac{1}{2}\frac{1}{\sqrt{1 - y_0}} \tag{C.6}$$

which is in the original variables

$$\epsilon_K(x_0) = \frac{1}{2}\frac{x_0}{\sqrt{h_K^2 - x_0^2}} \tag{C.7}$$

Appendix D. Solving for the Potential $u_{1,K}(x)$

We would like to solve the following integral equation

$$\ln \epsilon_K(x_0) = \int_0^{x_0(N_K)} \mathrm{d}x \, \frac{-u_{1,K}(x)}{\mathrm{d}x/\mathrm{d}s} \tag{D.1}$$

Substituting the brush path $x = x_0 \sin \omega_K s$ and changing variables to $U = x^2$ gives

$$\ln \epsilon_K(U_0) = \frac{1}{\pi}\int_0^{U_0} \mathrm{d}U \, \frac{-N_K \, u_{1,K}(U)}{\sqrt{U(U_0 - U)}} \tag{D.2}$$

Let us consider for a moment the operator Y such that

$$\mathrm{Y}[f(U')] = \int_0^{U'} \frac{\mathrm{d}U}{\sqrt{(U' - U)}}[f(U)] \tag{D.3}$$

where $f(U)$ is an arbitrary function. Let us apply this transform twice to a function $W(U)$ so that

$$\mathrm{Y}[\mathrm{Y}[W(U_0)]] = \int_0^{U_0} \frac{\mathrm{d}U'}{\sqrt{(U_0 - U')}} \int_0^{U'} \frac{\mathrm{d}U}{\sqrt{(U' - U)}} W(U) \tag{D.4}$$

Changing the order of integration and doing the integrals gives

$$\mathrm{Y}[\mathrm{Y}[W(U)]] = \int_0^{U_0} \pi W(U) \tag{D.5}$$

Let us rewrite eq D.2 so that

$$\ln \epsilon_K(U) = \frac{1}{\pi}\mathrm{Y}\left[\frac{-N u_{1,K}(U)}{\sqrt{U}}\right] \tag{D.6}$$

Then applying Y and using the relation given by eq D.5 we see that

$$\int_0^{U_0} \mathrm{d}U \, \frac{-N u_{1,K}(U)}{\sqrt{U}} = \int_0^{U_0} \mathrm{d}U \, \frac{\ln \epsilon_K(U)}{\sqrt{U_0 - U}} \tag{D.7}$$

Then we find $N u_{1,K}(U)$ by differentiating the right-hand side of eq D.7 with respect to U and multiplying by $U^{1/2}$. Using eq V.C.17 for the end density and changing variables back to x gives us eq V.C.18 where

$$\int_0^{h_K} \mathrm{d}x \, u_{1,K}(x) = 0 \tag{D.8}$$

Appendix E. Making the Expansion Parameter for the Brush Equations Obvious

In identifying an expansion parameter for eq III.5, we recognize that the brush height scales as h_K in order to maintain incompressibility, which implies a chain extension over N_K. Thus we scale the variables in the following way

$$\bar{x} = \frac{x}{h_K}, \qquad \bar{s} = \frac{s}{N_K}, \qquad \bar{u}_K = N_K u_K \tag{E.1}$$

The propagator equation becomes

$$\frac{\partial Q_K^{\mathrm{b}}}{\partial \bar{s}} = \frac{\delta}{6}\frac{\partial^2 Q_K^{\mathrm{b}}}{\partial \bar{x}^2} - \bar{u}_K(\bar{x}) Q_K^{\mathrm{b}} \tag{E.2}$$

where $\delta = N_K a/h_K^2$ as the small parameter, which is zero when $N_K \to \infty$. Then we use $Q_K^{\mathrm{b}}(\bar{x},\bar{s};\bar{x}_1) = \exp[-S_{0,K}/\delta - S_{1,K}]$ and so

$$-\frac{1}{\delta}\frac{\partial S_{0,K}}{\partial \bar{s}} - \frac{\partial S_{1,K}}{\partial \bar{s}} = -\frac{1}{6}\frac{\partial^2 S_{0,K}}{\partial \bar{x}^2} - \frac{\delta}{6}\frac{\partial^2 S_{1,K}}{\partial \bar{x}^2} + \frac{1}{6\delta}\left(\frac{\partial S_{0,K}}{\partial \bar{x}}\right)^2 + \frac{1}{3}\frac{\partial S_{0,K}}{\partial \bar{x}}\frac{\partial S_{1,K}}{\partial \bar{x}} + \frac{\delta}{6}\left(\frac{\partial S_{1,K}}{\partial \bar{x}}\right)^2 - \frac{1}{\delta}\bar{u}_{0,K} - \bar{u}_{1,K} \tag{E.3}$$

Separating terms order by order results in eqs V.A.5 and V.A.10.

References and Notes

(1) Bates, F. S. *Annu. Rev. Phys. Chem.* **1990**, *41*, 525.
(2) Leibler, L. *Macromolecules* **1980**, *13*, 1602.
(3) Semenov, A. N. *Sov. Phys. JETP (Engl. Translation)* **1975**, *61*, 783.
(4) Milner, S. T.; Witten, T. A.; Cates, M. E. *Macromolecules* **1988**, *21*, 2610.
(5) Hasegawa, H.; Tanaka, H.; Yamasaki, K.; Hashimoto, T. *Macromolecules* **1987**, *20*, 1651.
(6) Hashimoto, T.; Shibayama, M.; Kawai, H. *Macromolecules* **1980**, *13*, 1237.
(7) Richards, R. W.; Thomason, J. L. *Macromolecules* **1983**, *16*, 982.
(8) Matsen, M. W.; Schick, M. *Phys. Rev. Lett.* **1994**, *72*, 2660.
(9) Matsen, M. W.; Bates, F. S. *Macromolecules* **1996**, *29*, 1091.
(10) Almdal, K.; Rosedale, J. H.; Bates, F. S.; Wignall, G. D.; Fredrickson, G. H. *Phys. Rev. Lett.* **1990**, *65*, 1112.
(11) Whitmore, M. D.; Vavasour, J. D. *Macromolecules* **1992**, *25*, 5477.
(12) Hong, K. M.; Noolandi, J. *Macromolecules* **1981**, *14*, 727.
(13) Helfand, E.; Tagami, Y. *J. Chem. Phys.* **1971**, *56*, 3592.
(14) Helfand, E.; Wasserman, Z. R. *Macromolecules* **1976**, *9*, 879.
(15) Helfand, E. *J. Chem. Phys.* **1975**, *62*, 999.
(16) Helfand denotes the dividing surface by x_G.
(17) Semenov, A. N. *Macromolecules* **1993**, *26*, 6617.
(18) Matsen, M. W.; Schick, M. *Macromolecules* **1994**, *27*, 7157.
(19) Edwards, S. *Proc. Phys. Soc.* **1965**, *85*, 613.
(20) Feynman, R. P.; Hibbs, A. R. *Quantum Mechanics and Path Integrals*; McGraw-Hill: New York, 1965.
(21) Bender, C. M.; Orszag, S. A. *Advanced Mathematical Methods for Scientists and Engineers*; McGraw-Hill: New York, 1978; Chapter 10, p 484.
(22) Goldstein, H. *Classical Mechanics*; Addison-Wesley: Reading, MA, 1959.
(23) Street. *The Analysis and Solution of Partial Differential Equations*; Brooks-Cole: Monterey, CA, 1973; Chapter 9, p 304.
(24) Milner, S. T.; Wang, Z. G.; Witten, T. A. *Macromolecules* **1989**, *22*, 489.
(25) We see from eq V.D.2, that the correction terms become negative when $c_1 = h^2/N$, which is unphysical and might signal the limit of validity of the theory.
(26) Matsen, M. W. Personal communication.
(27) Whitmore, M. Personal communication.
(28) Leibler, L.; Witten, T. A.; Pincus, P. A. *Macromolecules* **1990**, *23*, 824.
(29) Orland, H.; Schick, M. *Macromolecules* **1996**, *29*, 713.
(30) Milner, S. T. *J. Chem. Soc., Faraday Trans.* **1990**, *86*, 1349.
(31) Netz, R. R.; Schick, M. *Europhys. Lett.* **1997**, *38*, 37.
(32) Ball, R. C.; Marko, J. F.; Milner, S. T.; Witten, T. A. *Macromolecules* **1991**, *24*, 693.
(33) Li, H.; Witten, T. A. *Macromolecules* **1994**, *27*, 449.

MA970377Y